HEALTH AND MEDICINE

Bacterioboat—A novel tool to increase the half-life period of the orally administered drug

Parmandeep Kaur[1], Sandip Ghosh[2], Arghya Bhowmick[3], Kundlik Gadhave[4], Satabdi Datta[1], Abhrajyoti Ghosh[3], Neha Garg[4,5], Roop L. Mahajan[6], Biswarup Basu[2]*, Diptiman Choudhury[1,6]*

The short half-life in the GI tract necessitates an excess of drugs causing side effects of oral formulations. Here, we report the development and deployment of Bacterioboat, which consists of surface-encapsulated mesoporous nanoparticles on metabolically active *Lactobacillus reuteri* as a drug carrier suitable for oral administration. Bacterioboat showed up to 16% drug loading of its dry weight, intestinal anchorage around alveoli regions, sustained release, and stability in physiological conditions up to 24 hours. In vivo studies showed that oral delivery of 5-fluorouracil leads to increased potency, resulting in improved shrinkage of solid tumors, enhanced life expectancy, and reduced side effects. This novel design and development make this system ideal for orally administrable drugs with low solubility or permeability or both and even making them effective at a lower dose.

INTRODUCTION

The oral route is the most convenient route of drug administration, and almost 80% of the drugs are administered through this route (*1*). Despite many advantages like self-administration, convenient, economical, pain-free, and noninvasive, oral route administration has serious challenges, especially for drugs (such as furosemide, cimetidine, enalaprilat, hydrochlorothiazide, inogatran, and losartan) with their characteristic low permeability through the gastrointestinal (GI) tract (*1*, *2*), leading to absorption of only 3 to 10% of the administered dose and reduced bioavailability (*3*, *4*). To overcome this challenge, the patient needs to take around 10- to 30-fold higher doses of the drug than the body requires, most of which comes out through feces without being metabolized. Use of excess drugs [such as isotretinoin, antibiotics, mycophenolate mofetil, rituximab, aspirin, and nonsteroidal anti-inflammatory drugs (NSAIDs)] may worsen various diseased conditions like irritable bowel syndrome, hemorrhoids, GI ulcers, cancer, Crohn's disease, and ulcerative colitis (*3*–*6*). In addition, mixing the unmetabolized drug with the environment like soil and drinking water causes biomagnification, leading to antibiotic resistance in microorganisms (*7*, *8*). Further, the use of the excess drug contributes to direct financial loss and an increase in health care costs. Various sustained-release formulations have been developed to solve these problems, which have helped increase bioavailability and reduce drug dosage (*6*–*9*). Liposome, micelles, and other nanoformulations provide a compelling advantage for better stability and solubility of drugs, especially in the hydrophobic and acidic milieu of GI fluid (*10*–*13*). However, upon oral administration, those formulations do not substantially increase the half-life period (30 to 60 min) in the stomach and the small intestine together (*9*, *12*). Earlier researchers have explored nanoparticle-coated bacteria for drug delivery purposes to mitigate these problems, where they have made microbots and attached nanoparticles to the bacteria through antigen-antibody interactions to deliver DNA-based model drug molecules inside the cells (*13*). In another study, researchers have used sugar-coated dextranomer microspheres on *Lactobacillus reuteri* to enhance probiotic activity (*14*).

In the present study, we have developed a novel, orally administrable cargo transport device named Bacterioboat (BB), using *L. reuteri*, a Gram-positive GRAS (Generally Recognized as Safe) bacterium that can carry and deliver cargo including drugs, small molecules, and macromolecules to the intestinal microvillus using biofilm, which is composed of a mixture of a variety of polysaccharides along with at least 40 different types of proteins including mucus-binding proteins (*15*, *16*). The polysaccharide-protein secretions of *L. reuteri* are actively absorbed by the microvillus of the intestine and aid its intestinal anchorage for days and sustained release of the drug. We hypothesized that this would increase the half-life period of the drug in the intestine and better bioavailability of drugs.

In a proof-of-concept study, a tumor-bearing mouse model was chosen to evaluate the efficacy of different doses of the oral anticancer drug 5-fluorouracil (5-FU) loaded into BB. Its effectiveness was compared to that of the conventional oral 5-FU treatment regime [50 mg/kg body weight (BW)] and a suboptimal dose regime (25 mg/kg BW). Further, bioavailability, change in drug potency, and side effects were compared with the conventional oral 5-FU treatment regime.

RESULTS

Synthesis and ultramicroscopic study of BBs

A schematic illustration of the synthesis procedure of BB is depicted in Fig. 1A. BB drug loading can be achieved using both in situ and ex situ methods. BB was prepared using chitosan by surface encapsulation with mesoporous nanoparticles on *L. reuteri*. Field-emission scanning electron microscopy (FE-SEM) studies showed smooth cell surface organization of freshly cultured control *L. reuteri* (Fig. 1B), whereas surface encapsulation of the bacteria with nanoparticles was observed in BBs (Fig. 1C). Magnification of surface nanostructures revealed the formation of sponge ball–shaped nanoparticles of 15 to

[1]School of Chemistry and Biochemistry, Thapar Institute of Engineering and Technology, Patiala, Punjab, India. [2]Department of Neuroendocrinology and Experimental Hematology, Chittaranjan National Cancer Institute, Kolkata, West Bengal, India. [3]Department of Biochemistry, Bose Institute, EN Block, Sector V, Bidhannagar, Kolkata, West Bengal 700091, India. [4]Indian Institute of Technology (IIT) Mandi, Mandi, Himachal Pradesh, India. [5]Department of Medicinal Chemistry, Faculty of Ayurveda, Institute of Medical Sciences, Banaras Hindu University, Varanasi, Uttar Pradesh, India. [6]Thapar Institute of Engineering and Technology–Virginia Tech (USA) Centre for Excellence in Material Sciences; Thapar Institute of Engineering and Technology, Patiala, Punjab, India.
*Corresponding author. Email: diptiman@thapar.edu (D.C.); biswarup.basu@gmail.com (B.B.)

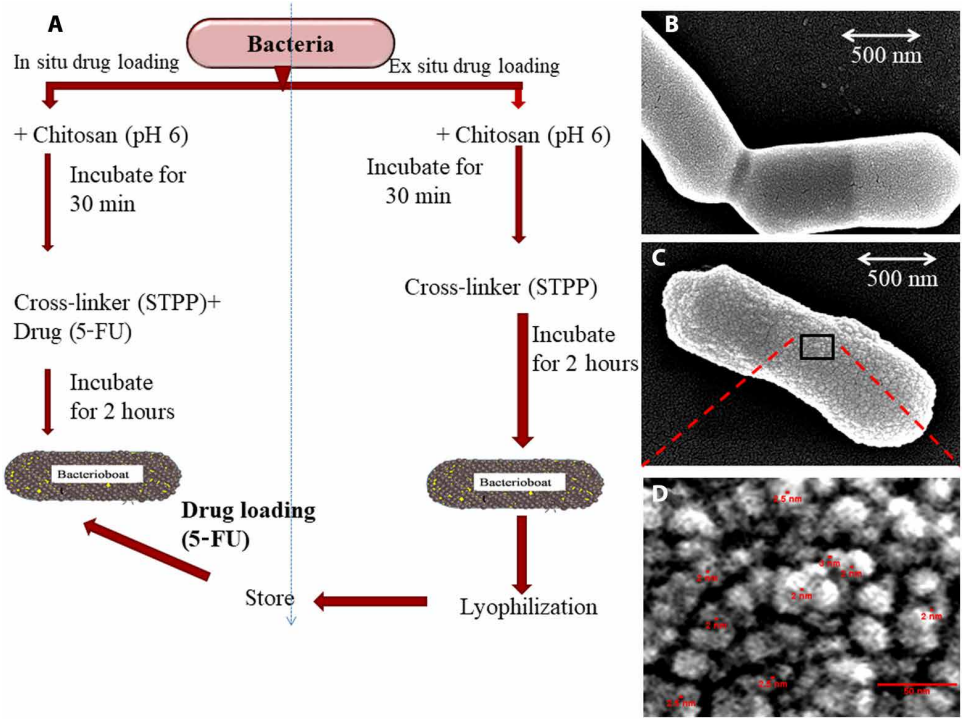

Fig. 1. BB synthesis and morphology. (**A**) Schematic representation of the synthesis of BB with in situ and ex situ loading protocol for drugs of choice. (**B**) FE-SEM image of *L. reuteri* cells. (**C**) FE-SEM image of freshly prepared BB showing chitosan nanoparticles on the cell surface. (**D**) Enlarged view of black box area of (C) illustrating the sponge ball–shaped nanoparticles of 15 to 25 nm in size with a pore diameter of around 2 to 3 nm.

25 nm diameter with mesopores of 2 to 3 nm diameter on the surface of BBs in lyophilized conditions (Fig. 1D and fig. S1).

Effect of BB formation on the growth of *L. reuteri*

To understand the effect of surface encapsulation on the cellular metabolism of *L. reuteri*, growth curve analyses were done. At the initial stage, a phase delay (elongation of lag phase) was prominent until 9 hours in BB, whereas in control it was between 3 and 6 hours. However, after 48 hours, a complete retrieval of the growth of BB was established (Fig. 2A).

Effect of BB formation on lactic acid metabolism

No significant changes in lactic acid production were observed compared to control *L. reuteri* upon surface encapsulation with mesoporous carbohydrate nanoparticles (Fig. 2B).

Biofilm producibility of BBs

The biofilm formation of *L. reuteri* was analyzed at different pH levels in MRS (De Man, Rogosa, and Sharpe agar) medium only and with enzymes present in the simulated gastric fluid (SGF) and simulated intestinal fluid (SIF). The increase in the biofilm formation in all the samples containing *L. reuteri* and BB with increasing time intervals is shown in Fig. 2 (C to E). It is shown from the data that comparatively among pH 2.0, 6.4, and 7.4, the biofilm produced is lowest at pH 2.0 for EBB (BB with enzyme) and is highest at pH 7.4 as compared to *L. reuteri* samples. FE-SEM images show the morphological comparison of the structure of *L. reuteri* and BB. The freshly cultured *L. reuteri* in a log phase of growth showed no biofilm formation (Fig. 2F), whereas 48-hour aged *L. reuteri* showed production of biofilm (Fig. 2G). The coating of mesoporous nanoparticles on the freshly cultured *L. reuteri* showed no biofilm formation (Fig. 2H). However, 48-hour aging of BB showed the formation of biofilm: BB with biofilm at pH 2.0, 6.4, and 7.4 at 48 hours after encapsulation aging (Fig. 2, I to K). The influence of chitosan concentration on biofilm production is shown in fig. S2. Biofilm production in the production capacity of *L. reuteri* and BB in simulated SGF and SIFs is shown in fig. S3 (A to D).

Stability of BBs and comparison of the growth curve of bacteria and BB

The stability of surface encapsulation is of utmost importance inside the intestinal environment to achieve increased half-life and sustained release. Therefore, the stability of BB was determined in SGF and SIF for up to 72 hours. Freshly prepared BB showed even the formation and distribution of surface nanoparticles (Fig. 3, A to C). Upon incubation, for 24 hours in SGF or SIF, no noteworthy changes in microscopically observable stability were found (Fig. 3, D to F). Secretory biofilm was observed in BB incubated in SIFs for 24 hours at both pHs, with more in pH 7.4 (Fig. 3, E and F). Subsequently, BB after 48 hours of incubation in SGF showed stability in the nanoparticle-encapsulated surface and a moderate increase in biofilm production (Fig. 3G). Whereas an extensive increase in biofilm formation along with little change in structural integrity was observed in Fig. 3H, BB was incubated with SIF at pH 6.4. However, BB, after incubation in SIF at pH 7.4, showed a change in surface morphology (Fig. 3I), with a huge enhancement of biofilm production. An overwhelming biofilm production resulted in the complete covering of the nanoparticle's encapsulated surface (Fig. 3I). After 72 hours of incubation,

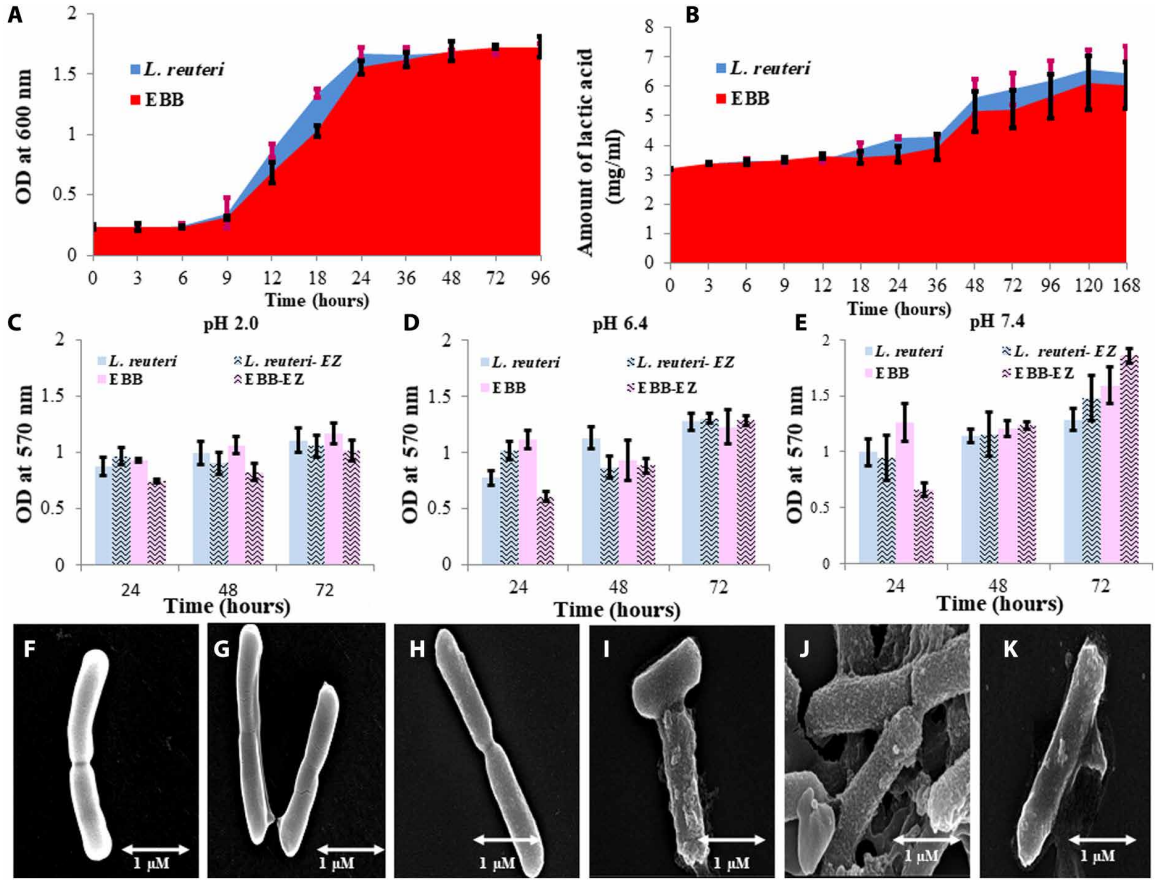

Fig. 2. Metabolic characterization of BBs. (**A**) Comparative cellular growth of *L. reuteri* (blue) and EBB (red). Because of cell wall encapsulation with mesoporous particles, the lag phase was extended. (**B**) Comparative lactic acid production (metabolic activity) efficiency between *L. reuteri* and EBB shows an insignificant efficiency alteration. (**C**) Comparative time depending on the study of biofilm production at pH 2.0 by BB and *L. reuteri* in SGF and SIF in the presence or absence of digestive enzymes. (**D**) Comparative time depending on the study of biofilm production at pH 6.4 by *L. reuteri* and BB in SGF and SIF in the presence or absence of digestive enzymes. (**E**) Comparative time depending on a study of biofilm production at pH 7.4 by *L. reuteri* and BB in SGF and SIF in the presence or absence of digestive enzymes. It has been found that in the absence of digestive enzyme, biofilm production gradually increased up to 72 hours. However, in the presence of a digestive enzyme (especially pancreatin), biofilm was reduced after the initial increase at 24 hours. This may have happened because of the amylase activity of the enzymes in SIF. (**F** to **K**) FE-SEM of (F) freshly cultured *L. reuteri* in log phase, (G) *L. reuteri* in 48-hour outraged culture (stationary phase), (H) freshly prepared BBs, (I) 48-hour SGF (pH 2.0) incubated BB, (J) 48-hour SIF (pH 6.4) incubated BB, and (K) 48-hour SIF (pH 7.4) incubated BB.

the partial disruption of the structure of the nanoencapsulated surface along with enhanced production of the biofilm was observed in SGF and SIF at pH 6.4 (Fig. 3, J and K). In SIF at pH 7.4, a complete disruption of the surface and swelling of the overall microbial structures were observed in Fig. 3L.

Effect of drug loading on bacterial growth and metabolism

5-FU is known for its growth-inhibitory effect on bacteria (*17*); therefore, the effect of 5-FU loading on BB was essential to understand. *L. reuteri* showed a prolonged lag phase up to 18 hours, and then, a slow recovery of the growth rate in the presence of 15 mg/100 mg (w/w) of the dry weight of *L. reuteri* was observed, although it could achieve only half of its maximum growth up to 96 hours, yet 5-FU–loaded BB (FUBB) [15 mg/100 mg (w/w)] resulted in a reduction of system toxicity in the mouse model, which may be due to sustained release of the same with reduction of the lag phase of *L. reuteri* up to 12 hours, followed by a faster recovery of the growth rate of *L. reuteri*. To understand the effect of surface encapsulation on the cellular metabolism of *L. reuteri*, growth curve analyses were done. At the initial stage, a phase delay (elongation of lag phase) was prominent until 9 hours in BB, whereas in control it was between 3 and 6 hours. However, after 48 hours, a complete retrieval of the growth of BB was established (Fig. 4A).

Effect of drug loading on lactic acid production

Lactic acid production was studied as a metabolic characteristic of the live bacteria in the drug-loaded BB. Around a 10% decrease in lactic acid production was observed due to the loading of 5-FU in BB compared to EBB (Fig. 4B).

Drug loading and release study in vitro at pH 2.0, 6.4, and 7.4

The efficiency of BB in ex situ drug loading conditions was higher (16.7 ± 1.6%) than that in in situ conditions (12.3 ± 2.4%). The mesoporous surface of the chitosan particles showed excellent absorptivity in saturated conditions. SGF and SIF showed sustained drug

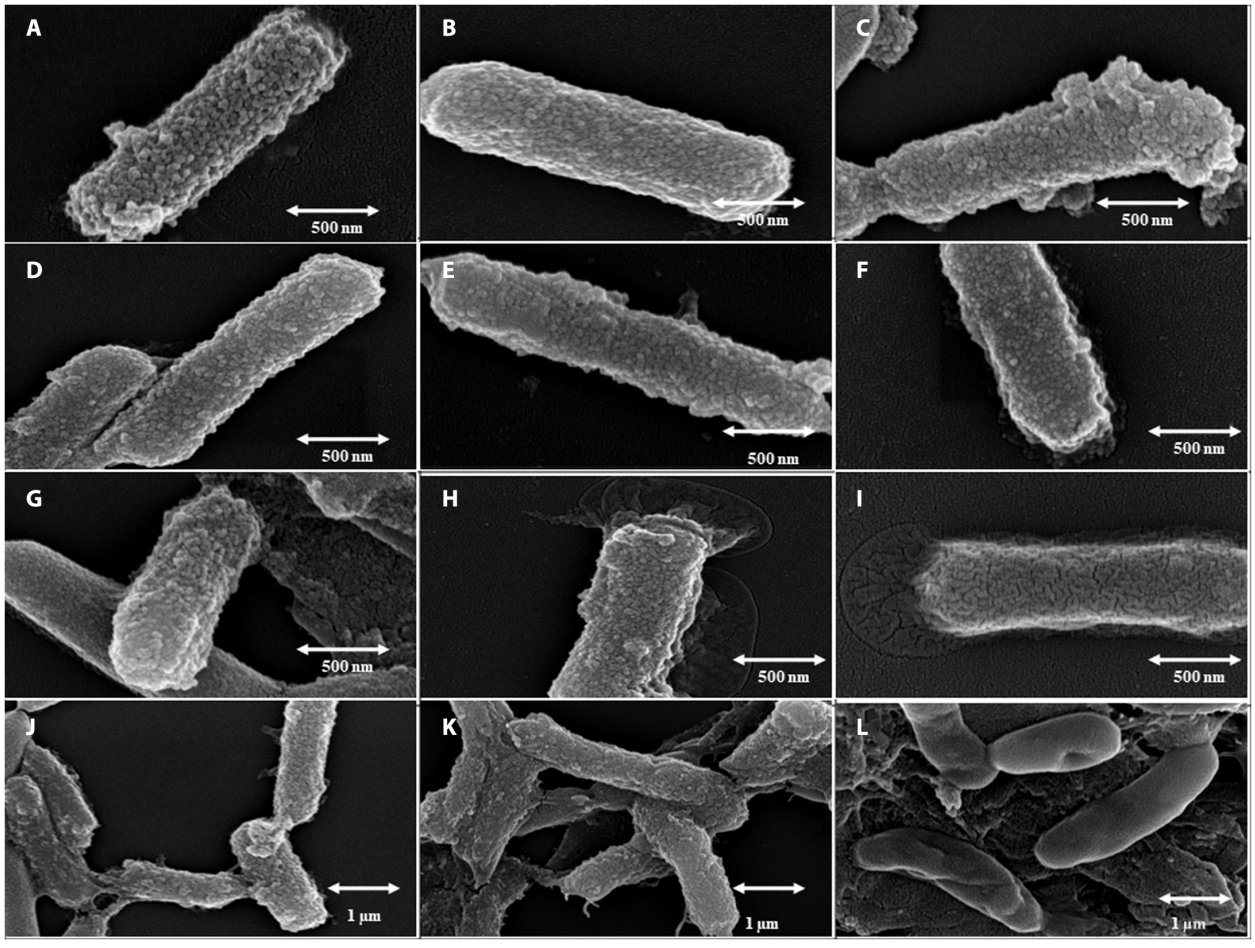

Fig. 3. Stability of the nanoparticle-encapsulated cell surface. FE-SEM images show the surface stability of BBs in SGF and SIF during drug release in the presence of digestive enzymes: (**A**) 0 hour in SGF at pH 2.0, (**B**) 0 hour in SIF at pH 6.4, (**C**) 0 hour in SIF at pH 7.4, (**D**) 24 hours in SGF at pH 2.0, (**E**) 24 hours in SIF at pH 6.4, (**F**) 24 hours in SIF at pH 7.4, (**G**) 48 hours in SGF at pH 2.0, (**H**) 48 hours in SIF at pH 6.4, (**I**) 48 hours in SIF at pH 7.4, (**J**) 72 hours in SGF at pH 2.0, (**K**) 72 hours in SIF at pH 6.4), and (**L**) 72 hours in SIF at pH 7.4.

release patterns from the nanoencapsulated surface. In SGF at pH 2.0, after an initial blast of drug release between 30 min and 1 hour, a sustained-release pattern was observed, and almost 98.43 ± 0.82% of drugs were released at 8.5 hours. In SIF, at both pH 6.4 and 7.4 after an initial blast, a sustained drug release was observed up to 97.6 ± 1.5% for 5.5 hours (Fig. 4C).

Confocal imaging, FE-SEM imaging, and fluorescence intensity comparison for intestinal anchorage by BB

The intestinal anchorage of BB on the mouse small intestinal sections ex vivo was monitored using confocal microscopy and FE-SEM (Fig. 5, A to D). BBs loaded with Rd (Rhodamine 123) were allowed to anchor on the GI tract of Swiss albino mice ex vivo. After incubation for 30 min, the intestine was subjected to confocal microscopy. Microscopic observation showed localization of BB around the alveoli of the intestine. Alveoli actively absorb biofilm's polysaccharides of BB, enabling them to adhere around the alveolar region (Fig. 5, A and B). The fluorescence of only Rd-treated small intestine (Fig. 5A) and *L. reuteri* in the mouse intestine section (Fig. 5C) was much less as compared to Rd-loaded BB in the mouse intestine (Fig. 5B) and the Rd-loaded BB on the alveolar regions of the mouse intestine (Fig. 5D). Likewise, the FE-SEM images of the mouse intestine (Fig. 5E) and BB anchored on the intestinal lining of mice (Fig. 5F) portray the anchorage of BB on the intestinal lining. A fluorescence intensity comparison assay was done in 96-well plate readers with only the intestine, only *L. reuteri*, EBB (empty BB), Rd-loaded BB on the intestine, Rd on the intestine, *L. reuteri* with Rd, and Rd-loaded BB. This assay depicted that fluorescence intensity was maximum in Rd-loaded BB on the intestine compared to Rd only, which indicates that BB has a good anchorage on the intestinal microvilli region and is deporting the dye in reasonable quantity and releasing it (Fig. 5G).

BB can attach to the wall of the murine intestine, and anchorage of FUBB leads to sustained release of the drug compared to direct 5-FU treatment in mice studied through liquid chromatography–electrospray ionization–mass spectrometry

To check the presence of *L. reuteri* getting attached to the mouse's intestine treated with FUBB, quantitative polymerase chain reaction

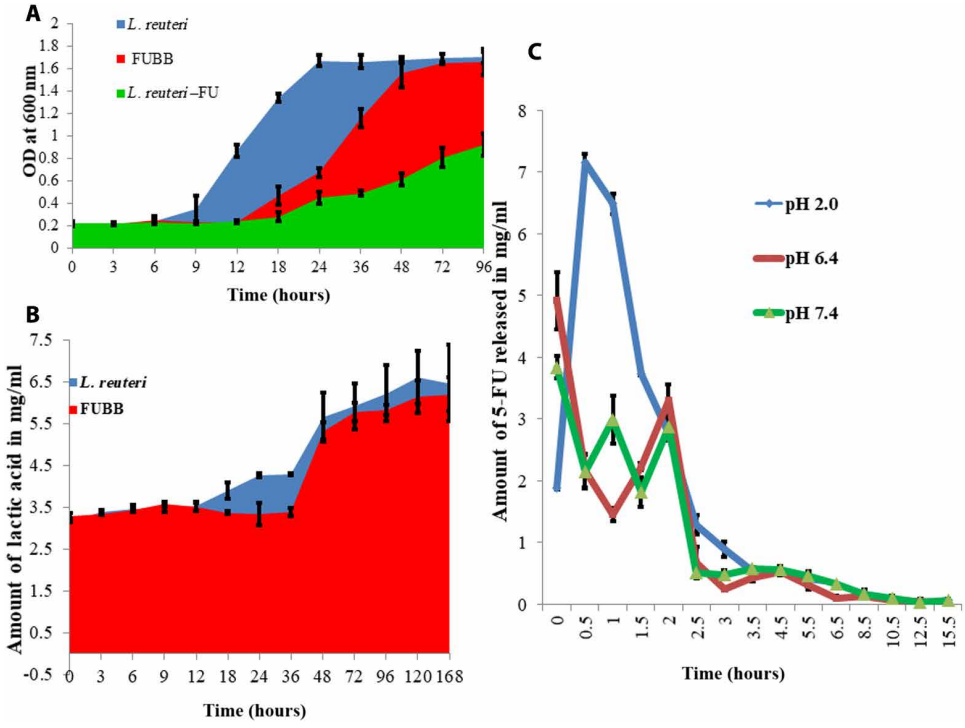

Fig. 4. Effect of 5-FU loading on BB metabolism and release of the drug. (**A**) Effect of growth on BBs due to loading of 5-FU. The drug prevented the growth of BB. FUBB (red) showed up to 12 hours of prolonged lag phase, whereas in EBB (blue) it was around 6 hours. 5-FU also caused a reduction of growth of *L. reuteri* (green), and the extent was higher than that of BB. (**B**) Lactic acid production (signature of *L. reuteri* metabolic activity), although it did not alter much due to 5-FU loading. (**C**) Release study of 5-FU after loading on BB in SGF at pH 2.0 (red), SIF at pH 6.4 (green), and SIF at pH 7.4 (blue). After the initial blast in SIF delayed blast in SGF (between 30 min and 1 hour), a sustained-release pattern was observed in all formulations.

(qPCR) analysis was performed, using genomic DNA (gDNA) extracted from the murine intestine samples. In Fig. 6A, qPCR analysis with *L. reuteri*–specific primers revealed that the abundance of the bacteria was around 10-fold higher in the case of the treated murine intestine sample compared to the untreated murine intestine 24 hours after oral gavage. All the mice used in these experiments were orally gavaged with antibiotics to reduce a load of nonspecific bacteria commonly found in their intestine. Because *L. reuteri* is a typical intestinal flora, the CT (cycle threshold) values for *L. reuteri*–specific genes were normalized against the universal 16*S* ribosomal DNA (rDNA), used as a reference. Our study shows that *L. reuteri* BB is efficiently getting attached to the wall of the murine intestine. In addition, comparative analysis of the presence of *L. reuteri*, BB, and FUBB (50 mg/kg) has been from the feces samples of treated mice for up to 24 hours. In all cases, a comparable amount of *L. reuteri* was found in the stool samples of mice. Figure S4 shows the comparative expression of 16*S* rDNA of *L. reuteri* in the feces of all three groups of mice at different time points (6, 12, and 24 hours) with *L. reuteri*–specific genes in the treated mice that were normalized against the universal 16*S* rDNA as a reference.

In the case of normal 5-FU treatment, Fig. 6B shows that the 5-FU drug persisted in the murine plasma sample for 5 hours, with the maximum abundance around 3 hours. After 8 hours, 5-FU drug abundance was found to decrease gradually. However, in the case of FUBB treatment, 5-FU drug abundance in the murine plasma sample was seen for almost 24 hours, although the $[M-H]^+$ abundance for 5-FU was less compared to direct 5-FU–treated murine plasma samples. This observation proves that FUBB acts as a better drug carrier, enabling the slow and sustained release of drugs compared to direct 5-FU treatment (*18*).

Effect of 5-FU with or without BB in tumor regression in vivo

Tumor volume was measured at 3-day intervals for each treatment group up to 29 days from the day of treatment onset, and data were graphically represented from three independent experiments (Fig. 7, A to D). Relative tumor volume on the 29th day was compared, and anti-tumor growth inhibition (TGI) was quantified as a percentage reduction from the control group. EBB-treated groups showed negligible TGI (9.98%) compared to the control group, and different doses of 5-FU treatment inhibited tumor growth differently [FU-25 (5-FU, 25 mg/kg BW) by 57.13% and FU-50 (5-FU, 50 mg/kg BW) by 77.69%]. FUBB-25 (FUBB, 25 mg/kg BW) treatment inhibited tumor growth by 74.19%, whereas FUBB-50 (FUBB, 50 mg/kg BW) treatment showed the highest TGI (90.29%, i.e., 12% higher treatment benefit from the FU-50–treated group) than the control group. BB strategy achieved treatment benefit to FUBB-25 and FUBB-50 groups in terms of higher efficacy than FU-25 and FU-50 groups.

Tumor reduction was found to be almost equivalent for FU-50– and FUBB-25–treated groups, inferring that 5-FU at 50% low dose with BB is as effective as 5-FU at conventional dose. Figure 7A shows S180 (sarcoma 180) solid tumors in all groups on the 29th day of treatment. Figure 7B shows relative tumor volume over the treatment period. The data show a distinguishable difference among

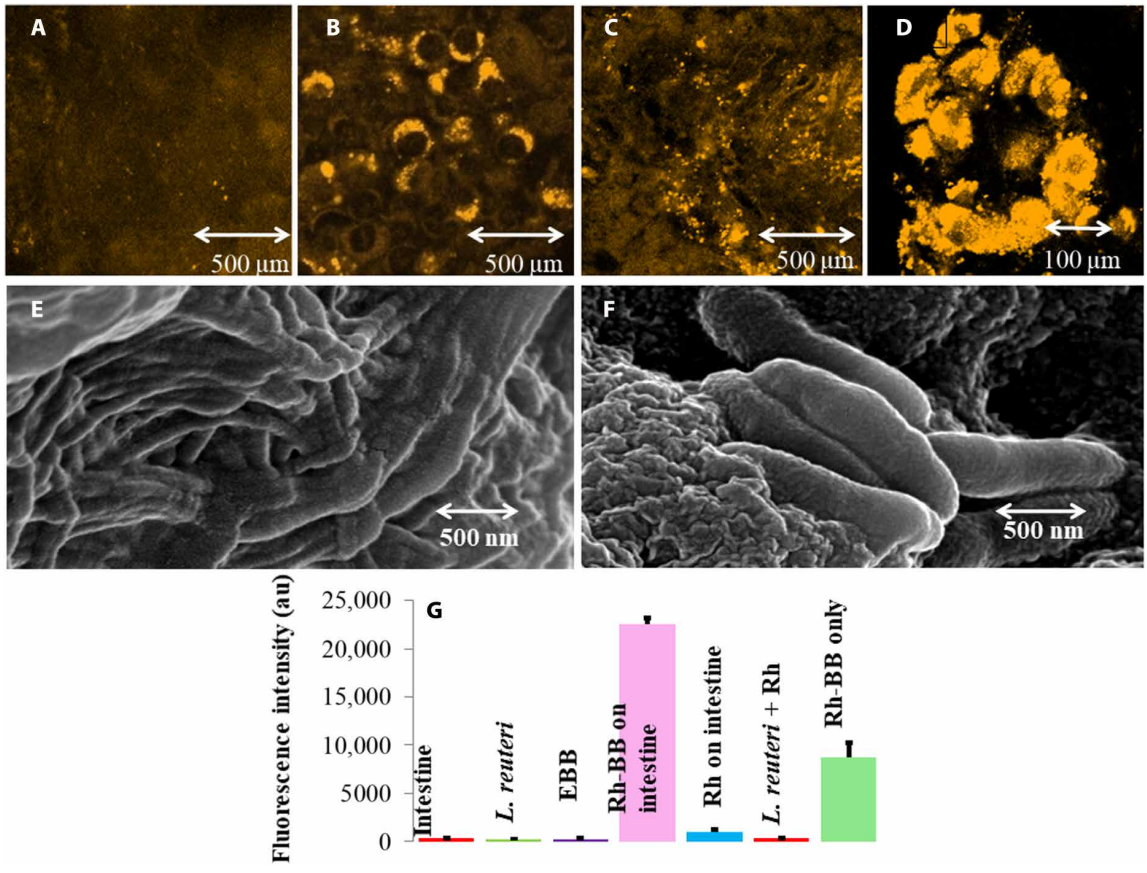

Fig. 5. Anchorage of BB on the intestinal surface (ex vivo). Confocal images for a BB anchorage on the intestinal surface. (**A**) Rd-treated mouse intestine. (**B**) Rd-loaded BB anchored around the alveolar regions of the mouse intestine. (**C**) *L. reuteri* treated with Rhodamine on the intestine. (**D**) BB treated with Rhodamine attachment on the intestine (magnified view). (**E**) FE-SEM image of cleaned mouse intestine showing clear projections of the mouse intestine. (**F**) FE-SEM image of BB anchored on the mouse intestinal lining. (**G**) Comparative fluorescence intensity detection using a 96-well plate by BB loaded with fluorescent dye Rd on mouse intestinal tissue shows maximum fluorescence with the Rd-loaded BB on the intestine after Rd-loaded BB directly on the polystyrene plate well, while the other shows the least fluorescence. au, arbitrary units.

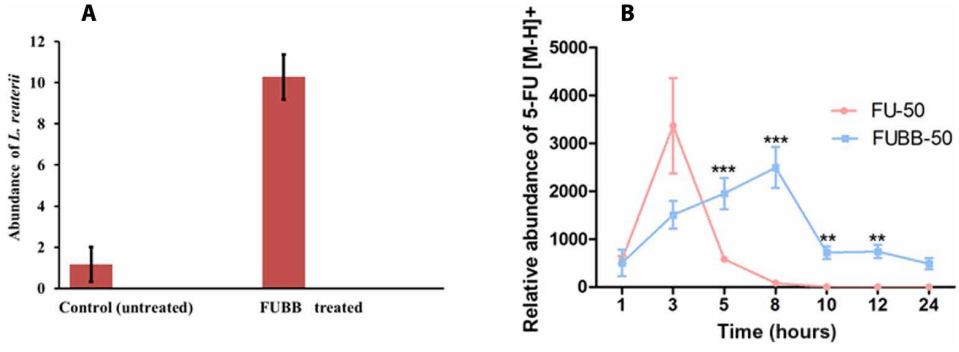

Fig. 6. Stability of BB in the mice in vivo using RT-PCR and bioavailability of 5-FU in the plasma of treated mice using LC-ESI-MSAB. The relative abundance of *L. reuteri* detected by reverse transcription PCR (RT-PCR) and the relative abundance of 5-FU [M-H^+] were plotted as means ± SE at different time points concerning the untreated murine plasma, which served as a control. () RT-PCR data show the presence of *L. reuteri* in the mouse intestine, as the signal for the FUBB-treated mice is 10 times than the control even at 24 hours after administration. () Detectable amount of the 5-FU drug in the mouse plasma up to 8 hours when applied alone using the oral delivery route and detectable amount of 5-FU delivered orally using FUBB up to 24 hours (**$P < 0.01$ and ***$P < 0.001$).

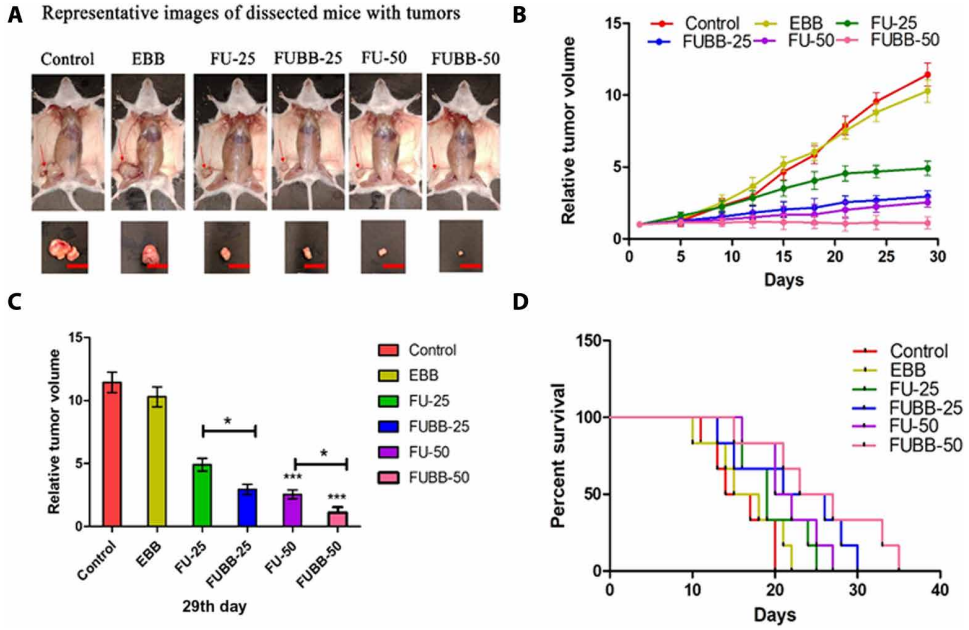

Fig. 7. In vivo validation of the efficacy of BBs. (**A**) S180 solid tumors in all groups were photographed immediately after euthanization (the 29th day of treatment). The red color scale bar shows 1 cm of the length of the S180 tumor shown in the euthanized mice. (**B**) The relative tumor volume of mice in different treatment groups is graphically represented. (**C**) Relative tumor volume on the 29th day. Values indicate means ± SD ($n = 6$). *$P < 0.05$, **$P < 0.01$, and ***$P < 0.001$. (**D**) Survival benefits among different groups are represented following Kaplan-Meier analysis of S180 ascites tumor-bearing mice.

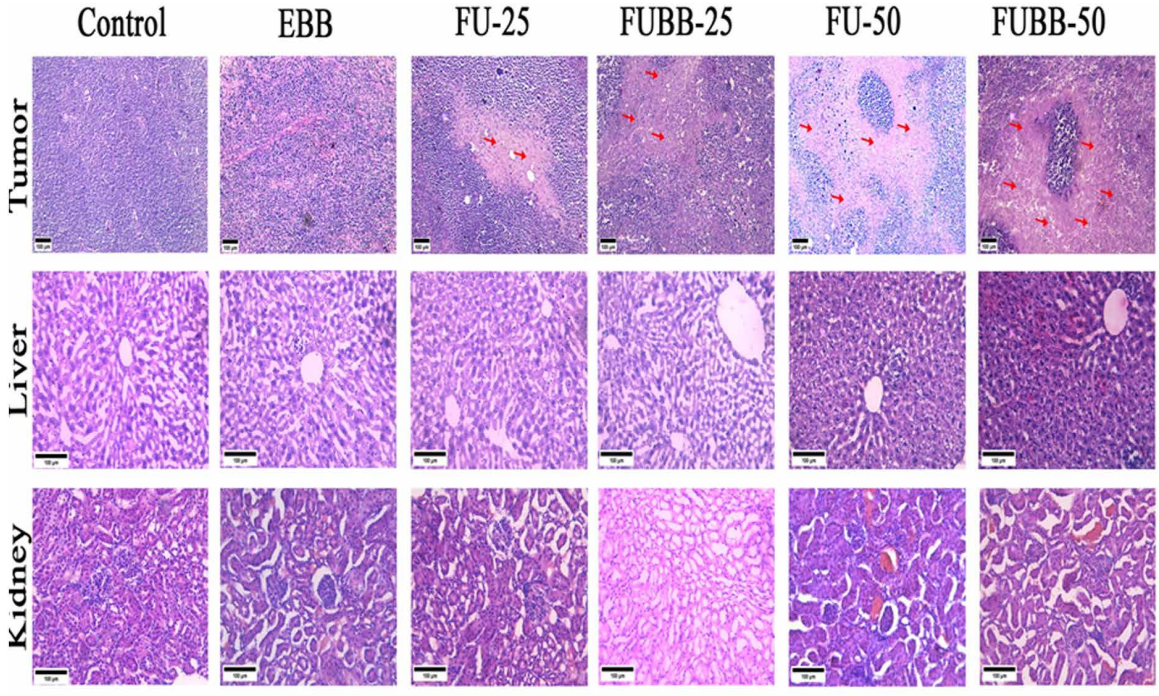

Fig. 8. Photomicrograph of S180 tumor, liverand kidney (H&E-stained). H&E staining of sections from S180 solid tumor (×100 magnification), liver (×200 magnification), and kidney (×200 magnification) shows tumor architecture in different treatment groups and the effect of treatment in vital organs. Red arrows in tumor histology indicate necrotic areas.

the relative tumor volume of the control 5-FU–treated tumor versus FUBB-treated tumor. In the case of a newly developed system, better tumor reduction was observed. Figure 7C shows a graphical representation of the relative tumor volume on the 29th day of treatment, implying the treatment's effectiveness with BB.

Survivability of tumor-bearing mice

Posttreatment survival benefits of tumor-bearing mice were obtained from Kaplan-Meier analysis of data of animal survival at the end of the study. The median survival values were listed as 15.5, 16.5, 19, 23.5, 21, and 25 for control, EBB, FU-25, FUBB-25, FU-50,

and FUBB-50 groups, respectively (log-rank $P = 0.0343$, $\chi^2 = 12.04$) (Fig. 7D).

Histopathological analysis of tumor and other vital organs following treatment

Tissue architecture changes were obtained from the histopathological analysis by hematoxylin and eosin (H&E) staining (Fig. 8). Hematoxylin is a DNA binding dye converting nuclei into blue or purple color, while cytoplasm or stromal parts remain pink by eosin. Tumor tissue morphology in control and EBB was characterized by well-organized and high-density nuclei and no visible necrosis. Noticeable tumor necrosis and reduced nuclei density were observed in the FU-25 group. FUBB-25 and FU-50 groups showed higher tumor necrotic areas and decreased tumor nuclei than the FU-25 group, but both have shown nearly similar results. The FUBB-50 group has shown substantial higher necrotic areas and nuclei density among all groups. Histopathological analysis of liver and kidney sections was also carried out in all groups to understand any toxicity-related changes due to treatment. EBB, FU-25, and FUBB-25 groups showed normal hepatocyte structure and prominent central vein without any sign of cytoplasmic degeneration and necrotic foci, but FU-50 and FUBB-50 have shown sinusoidal destruction. In kidney sections, all groups showed normal glomerular architecture with abundant tubule and capsular space, and no toxicity features like necrotic foci, leukocyte infiltration, and distorted glomeruli were observed.

Biochemical evaluation

Blood serum analysis on the 29th day from each group for liver enzymes [serum glutamic oxaloacetic transaminase (SGOT) and serum glutamic pyruvic transaminase (SGPT)] and other biochemical parameters (albumin, alkaline phosphatase, bilirubin, cholesterol, triglycerides, globulin, creatinine, liver weight, and BW of test mice) was graphically represented (Fig. 9). Elevated values of almost all parameters were observed with the increase of 5-FU doses (FU-25 and FU-50). Treatment with FUBB-50 reduced these, whereas treatment with the FUBB-25 dose significantly decreased these parameter values. For all parameters, E.B treatment showed a negligible change of values compared to the control groups. Analysis of statistical data is given in tables S1 to S22.

Host immune response against BB-mediated drug delivery

The blood cell count from serum significantly changes the treatment group compared to the control. However, no significant differences were observed between the FU-50 and FUBB-50 groups [Fig. 9 (L to N) represents the count of leukocytes, red blood cells, and platelets, respectively]. Further, proinflammatory interleukin-6 (IL-6) level analysis by enzyme-linked immunosorbent assay (ELISA) revealed that, due to the treatment, a considerable change took place in the IL-6 level in comparison with control when treated with 5-FU, but no significant difference was observed between the FU-50 and FUBB-50 groups (Fig. 9O). For anti-inflammatory response (IL-10), a slight increase was observed in the treatment groups compared to the control. However, the difference was not significant enough for any set at 5 days after treatment (Fig. 9P).

DISCUSSION

Devising a universal drug delivery system that can deliver many drugs through the oral route with an increase in the drug's half-life in the intestinal region is quite challenging. We have hypothesized to develop an oral delivery method that will show sustained cargo release in the GI track with a superior half-life period in the GI tract. Here, we have used metabolically active *L. reuteri* for this purpose. Metabolically active *L. reuteri* secretes biofilm in the gastric and intestinal conditions, allowing them to adhere to the microvilli's intestinal surface. A conclusive schematic representation demonstrating the advantages of the BB system in terms of intestinal anchorage and sustained release of drug is presented in Fig. 10. qPCR analysis with *L. reuteri*–specific primers revealed that the abundance of the bacteria was around 10-fold higher in the case of the treated murine intestine sample compared to the untreated murine intestine. We have further used cell wall encapsulation using mesoporous carbohydrate nanoparticles, which can absorb a variety of molecules (such as drugs and dye) released in a sustained manner around the microvilli, resulting in efficient intestinal absorption of the drug. Enhanced and prolonged absorption resulted in an increase in the bioavailability of the drug in vivo. We have shown that the formulation can increase the bioavailability of 5-FU up to 24 hours when applied through BB compared to the conventional oral dose where the traces of the drug was detectable in the serum only up to 8 hours. An increase in bioavailability also resulted in the requirement of administrable drug doses. Solid tumor size reduction and animal serval data suggested that even at half of the recommended dose, the comparable (with recommended dose) tumor size reduction was observed when the drug was applied through BB, which resulted in better animal survival. The animal showed 10% enhanced survival when half of the recommended dose was applied through BB compared to the recommended dose, which may happen because of the reduction of the drug-related side effects. 5-FU is reported to cause a considerable increase in hepatic fat content, resulting in frequent hepatic steatosis in patients. Therefore, it would be interesting to know how applying drugs through BB resulted in liver damage and serum fat accumulation. Different parameters including SGOT, SGPT, albumin, globulin, alkaline phosphatase, liver weight, and BW analysis showed a noticeable reduction of drug-related liver toxicity. Further, FUBB showed a noticeable reduction of drug-induced serum cholesterol and triglyceride level. Since the 1990s, the U.S. Food and Drug Administration (FDA) approved many drugs with nanoformulations that were reported to be more effective and had fewer side effects compared to the drugs that are available in the market. For example, Doxil/Caelyx (Janssen) liposomal doxorubicin (PEGylated) was approved by the FDA in 1995 and the European Medicines Agency (EMA) in 1996; recently, liposomal formulations of cytarabine by Jazz Pharmaceuticals were approved by the FDA (2017) and EMA (2018) (*11*). These formulations have several side effects like trafficking of the nanoparticles in the lymph nodes or bloodstream and the nanoparticles themselves having stability and toxicity issues and are mostly given through the intravenous route. As per the present system, chitosan nanoparticles remain in the gut (chitosan being a nontoxic, biodegradable, carbohydrate-based polymer used to form the nanoparticles over the surface of GRAS bacteria *L. reuteri*). *L. reuteri*, which have a probiotic potential and a normal inhabitant of the gut, was used as a vehicle as EBB. Further, it is possible to generate BB with other bacteria, such as *Acinetobacter catcoacetlus*, *Escherichia coli*, *Bacillus subtilis*, and *Lactobacillus rhamnosus* (fig. S5), and may be explored for drug delivery and other purposes. BB can be stored after lyophilization and loaded with various drugs without changing the drug's chemistry, making them

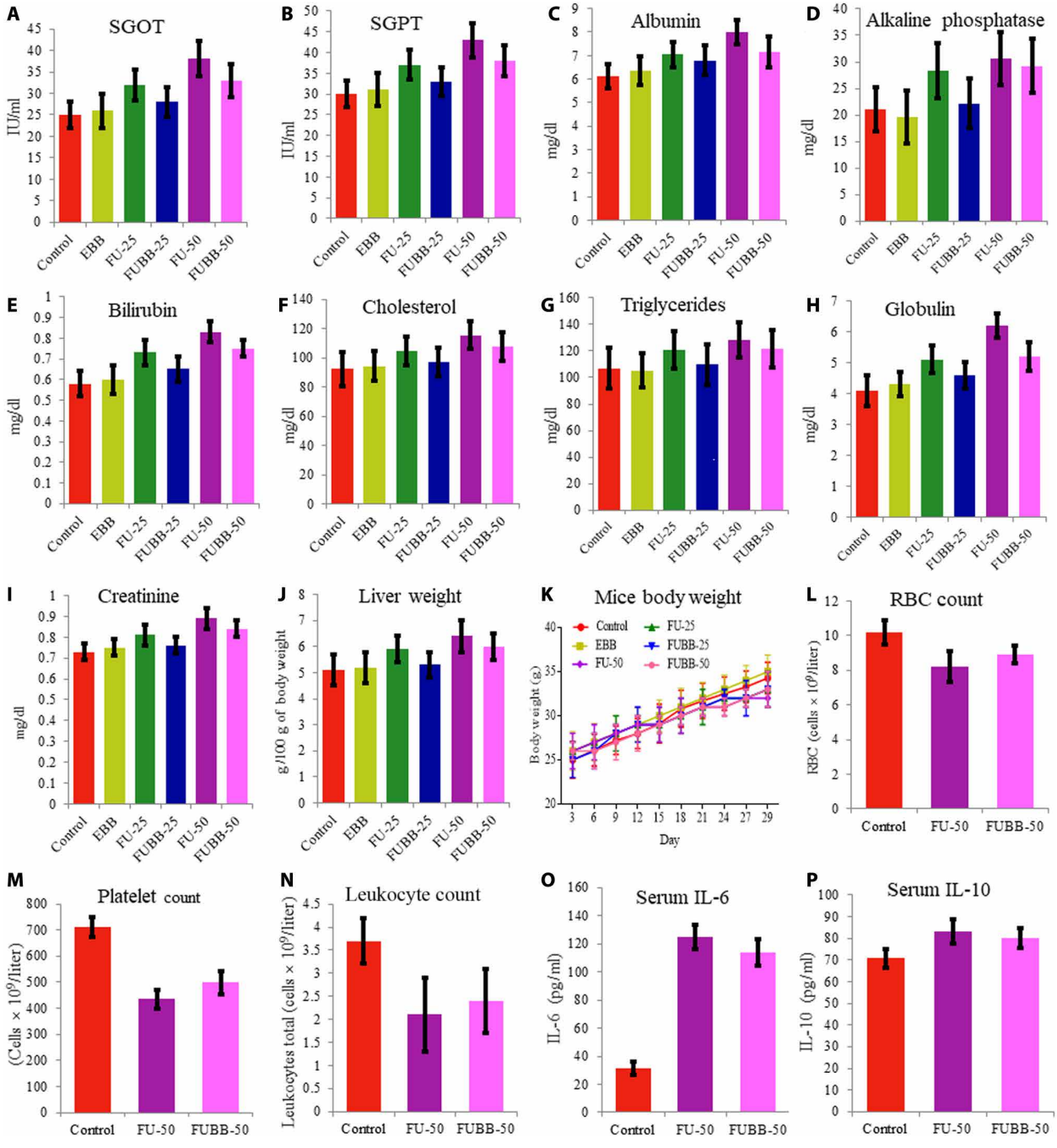

Fig. 9. Toxicity profiling and host immune response due to administration of 5-FU using BB. To determine the toxicity profile, serum samples were taken from different treated groups for (**A**) SGOT, (**B**) SGPT, (**C**) albumin, (**D**) alkaline phosphatase, (**E**) bilirubin, (**F**) cholesterol, (**G**) triglycerides, (**H**) globulin, (**I**) creatinine, (**J**) liver weight, and (**K**) BW of the mice during the murine sarcoma (S180) treatment in the in vivo experiment. Further, to determine the immune response against the novel delivery system, Swiss albino mice were treated with FU-50 and FUBB-50, and cell count and cytokine concentrations were determined from whole blood. The total count of blood cells is represented in (**L**) to (**N**): (L) leukocyte, (M) red blood cell (RBC), and (N) platelet counts. (**O** and **P**) Both proinflammatory cytokine (IL-6) and anti-inflammatory cytokine (IL-10) are represented. Data were taken from three independent experiments and plotted with their means ± SD.

an ideal candidate vehicle for oral drug delivery. In addition to that, BB does not considerably alter the body's immune response. Despite many advantages of intestinal drugs, absorption might have limited application for slightly acidic drugs that primarily get absorbed by the stomach, as low stomach pH is unfavorable for BB to bind. However, its surface coating has shown excellent sustained-release property at the SGF, suggesting that BB made with suitable bacteria such as *Prevotella* spp., *Streptococcus* spp., and *Veillonella* spp. is among the other viable options for this purpose. Further, because the bacteria are metabolically active, its

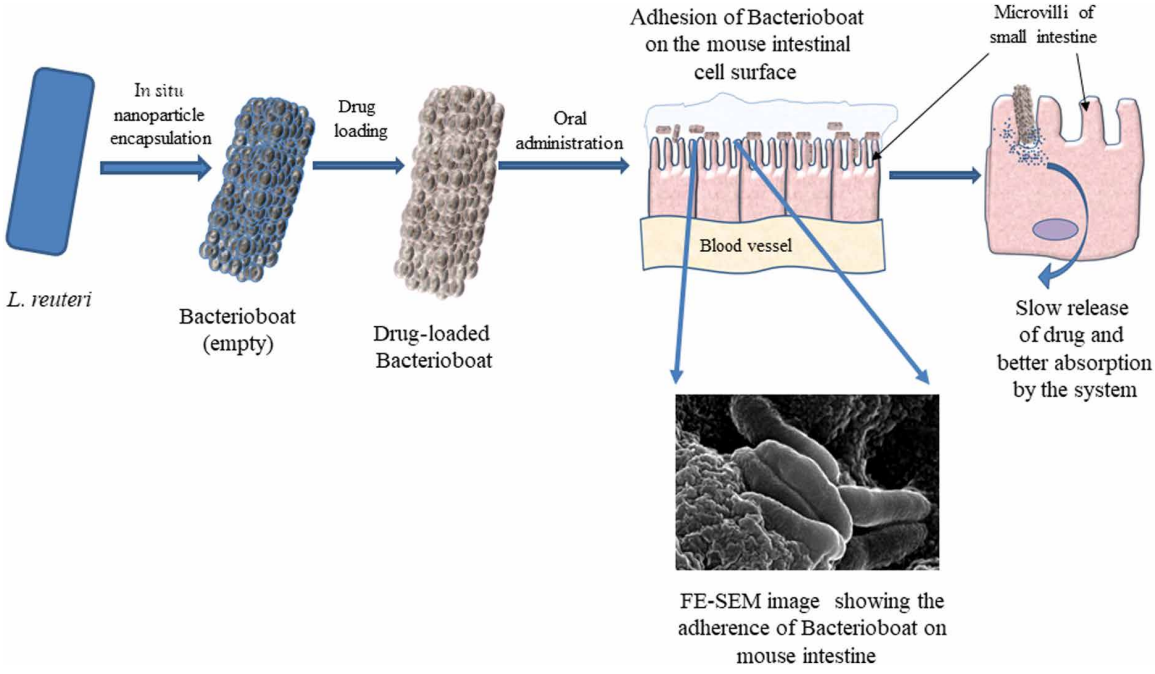

Fig. 10. Representation of BB attachment on the intestinal lining. The schematic illustration shows the intestinal anchorage of BB and sustained intestinal release and enhanced absorption of the drug for the orally administered BB system.

application through alternative routes, such as intravenous, intramuscular, and intradermal, is limited. At this point, further exploration and evolution are needed in preclinical and clinical trials to understand its true futuristic potential for clinical application.

MATERIALS AND METHODS

Materials

Chitosan, pepsin, potassium monophosphate monobasic, dialysis membrane, $CuSO_4$, sulfuric acid, glacial acetic acid, and ethyl acetate were purchased from HiMedia, India. Sodium tripolyphosphate (STPP), pancreatin, 5-FU, orthophosphoric acid, glacial acetic acid, trichloroacetic acid, and Rd were purchased from Merck (previously Sigma-Aldrich) in the United States. Formic acid, acetonitrile, and *p*-hydroxydiphenyl were purchased from Loba Chemie. All the reagents used were of analytical grade.

Culturing and maintenance of *L. reuteri*

L. reuteri (strain no. UBLRu87) was purchased from Unique Biotech Company. The bacteria were cultured in 1× MRS medium at pH 6.5 and 37°C. Then, it was plated to grow and isolated from a single colony in MRS agar. Then, the single colony was picked from it and inoculated in MRS medium at pH 6.5 and 37°C and incubated for 48 hours. Freshly grown culture (0.5 ml) was added to 0.5 ml of 40% glycerol to a cryogenic vial, gently mixed, and vortexed. Freshly cultured *L. reuteri* were frozen at −80°C in 40% of glycerol to maintain the stock.

Synthesis of BBs

Mesoporous carbohydrate nanoparticles were synthesized on *L. reuteri* following our protocol. At first, 1% chitosan stock solution was prepared by dissolving crystalline chitosan in 85% *o*-phosphoric acid solution at pH 6 under constant stirring at 120 rpm for 2 hours at 50°C temperature. Then, freshly grown and harvested *L. reuteri* cells were washed thrice using phosphate buffer (pH 7.0) to remove residual medium and other debris. Cleaned cells (~16×10^8 cells/ml) [optical density (OD) 2.0] were then suspended in 0.05% chitosan solution (pH 6) and incubated for 30 min at room temperature. After incubation, 1 mg/ml of STPP (40 ml for each 100 ml) as cross-linker was added to the solution dropwise with constant stirring at 60 rpm at room temperature. The mixture was kept under stirring condition for 2 hours to complete the reaction. After the response was over, the microbial cells were harvested and cleaned using phosphate-buffered saline (PBS) buffer at pH 7.0 (two times) before further processing. Processed and cleaned cells (BBs) were pelleted down by centrifugation at 1500 rpm and then were lyophilized for further use. The scheme of the synthesis of BBs is presented in Fig. 1A (*19*).

Characterization of BBs

Morphological characteristics of thus formed BBs were elicited using FE-SEM. Freshly prepared *L. reuteri* cells and BB samples (1×10^5 cells) were centrifuged at 5000*g* for 10 min, and the pellet was then suspended in 100 mM PBS (1.0 ml) buffer (pH 7.0). The cells were then fixed using 3% glutaraldehyde solution in PBS for 3 hours at 4°C. After fixation, cells were harvested by centrifugation at 5000*g* for 10 min, and thus obtained pellets were washed with 50 mM buffer twice before resuspending them in the same buffer (1.0 ml). Ten microliters of the suspension from each tube was placed separately on cleaned silicon wafers (grids) and incubated for 45 min at room temperature in the humidified chamber. The samples were then dehydrated using 50, 70, 95, and 100% ethanol

gradient for 10 min each. After dehydration, the sample grids were coated with 10-nm gold using the electrosputtering method. Last, the size, shape, mean diameter, and pore diameter of nanoparticles and the size distribution and morphology of *L. reuteri* and BBs were analyzed using SEM (Nova Nano SEM-450, FEI).

The surface potential of BBs

L. reuteri develops negative potential at low pH, and chitosan develops a positive one; therefore, at low pH, chitosan will interact with the bacterial cell wall, and upon applying STPP as a cross-linker, it can improve stabilization of the system. Therefore, the zeta potential of the bacteria before and after the formation of BBs was determined using Zetasizer (Nano Series Nano-ZS, model ZEN 3600, Malvern Instruments Limited). A zeta potential of −30.3 ± 3.57 mV of *L. reuteri* was turned into +5.39 ± 0.54 due to the formation of EBBs. The zeta potential of 5-FU–loaded (ex situ) BBs further changed into +17.62 ± 0.59, −0.74 ± 0.63, and − 5.8 ± 1.2 for pH 2.0, 6.4, and 7.4, respectively.

In vitro loading of the drug on BBs

For this work, 5-FU, a pre-pro-drug of 5-FU, has been used as a standard drug to demonstrate the delivery system's efficiency. 5-FU has a half-life of 8 to 20 min in the GI tract, which has been increased to 45 min by chemical modification and is in medical use for treating various cancers like colorectal, breast, esophageal, gastric, neuroendocrine, pancreatic, and ovarian. Two mutually independent strategies were taken to achieve drug loading, namely, in situ and ex situ loading. For in situ loading, the saturated solution of the drug for 5-FU (26 mg/ml) along with STPP (1 mg/ml) was added dropwise to the chitosan preincubated *L. reuteri* (5×10^8 cells/ml), and the solution was kept under constant stirring (at 60 rpm) for 2 hours to form drug-loaded BBs. After incubation, the drug-loaded BBs were harvested by spinning (1500 rpm), quickly washed twice with 1× PBS to remove excess materials, and lyophilized for storage for further use. For ex situ drug loading, lyophilized BBs (5×10^8 cells/ml) were suspended and incubated in 5-FU (26 mg/ml) solution for 2 hours at room temperature. The drug-loaded BBs were processed as before. The drug encapsulation efficiency (EE, %) of drugs that were entrapped into the nanoparticles was calculated using Eq. 1, and the drug loading capacity (LC), the ability of nanoparticles to in-trap drugs by nanocarrier dry weight, was determined by Eq. 2 (*20*, *21*)

$$\text{EE}\,\% = [(\text{Total drug} - \text{Free drug})/\text{Total drug}]*10 \quad (1)$$

$$\text{LC}\,\% = [(\text{Total drug} - \text{Free drug})/\text{Nano-carrier dry weight}]*100 \quad (2)$$

Drug release study in vitro from drug-loaded surface-encapsulated nanoparticles

In vitro drug (5-FU) release studies were performed in SGF and SIF. The composition of SGF was 0.03 M NaCl, 0.2 M HCl, and 3.2 g of purified porcine pepsin per liter of the buffer (pH 2.0) (*22*). Further, two SIF preparations were prepared, one with pH 6.4 and the other with pH 7.4. Both had 0.05 M monobasic potassium phosphate, 0.015 M sodium hydroxide, and 1 g of purified porcine pancreatin (w/w) per liter of the buffer (*21*). Drug-loaded lyophilized BBs (200 mg) were suspended in 1 ml of SIF or SGF and loaded in dialysis bags (12 kDa cutoff), and the samples were placed in 10 ml of the same buffer as before and incubated at 37°C in a constant stirring condition at 60 rpm for 15 hours. The samples were collected at different time points until 15 hours in each interval. The data obtained were plotted and calculated against the standard curve made using known concentrations of drugs in the respective buffer following its characteristic ultraviolet-visible absorption peak at 241 nm (*23*).

Metabolic characteristics of BBs in drug-unloaded and drug-loaded conditions

To study the effect of BBs on the lively activity of *L. reuteri*, further characterizations were done.

Effect of BB formation in the bacterial growth curve

To see the effect of surface encapsulation of *L. reuteri* on the metabolic activity, bacterial growth curve analysis followed by the doubling time analysis was done for *L. reuteri*, EBBs, FUBB, and 5-FU + *L. reuteri*. Systems were incubated for 168 hours at 37°C at 120 rpm, and OD was collected from time to time at 600 nm. Initial inoculum for *L. reuteri*/BBs was taken (100 mg), and 5-FU (0.1 mg) was loaded on BBs or incubated with *L. reuteri*.

Effect of BB formation on lactic acid production

The name *Lactobacillus* is given because of the ability to produce secretory lactic acid by the genus of bacteria. Therefore, lactic acid production is chosen as their signature metabolic activity parameter. It was studied to check any metabolic activity alteration due to the BB formation or drug loading. To culture, *L. reuteri* or BB whey was used as the medium. While boiling, whey was prepared from skimmed milk by glacial acetic acid (0.3 ml/liter). After cooling, whey was separated by centrifugation at 8000*g* for 5 min to remove the remaining proteins, and pH was adjusted to 6.0. Sterile whey medium (25 ml) was inoculated with (~1.6×10^6 cells/ml) *L. reuteri*, EBBs, and FUBB and incubated at 37°C for 168 hours at 120 rpm. Samples were isolated at different time points and were estimated using modified Barker and Summerson's method (*24*). In short, after removal of cells by centrifugation at 16,000*g* for 5 min, 100 μl of trichloroacetic acid was added per 1 ml of clear supernatant and incubated on ice for 30 min. Then, the precipitate was removed by centrifugation at 16,000*g* for 5 min, and the clear solution (A) was diluted using a 2% (w/v) $CuSO_4$ solution. After that, 1 g of $Ca(OH)_2$ was added per 10 ml of the sample solution (A). In this condition, the mixture was incubated at 37°C for 30 min, followed by precipitation removal by centrifugation at 16,000*g* for 5 min. Incubation in a boiling water bath for 5 min of the sample was done after the addition of 50 μl of 4% (w/v) $CuSO_4$ and 6 ml of concentrated H_2SO_4 per milliliter of solution A. After cooling, 0.1 ml of *p*-hydroxydiphenyl (0.2 M, pH 10) was added per milliliter of solution A and incubated at 30°C for 30 min. Last, the absorbance was taken at 570 nm and plotted against the standard sodium lactate solution to determine the concentration (*24*).

Effect of the biofilm production in the presence of different chitosan concentrations

Biofilm, a mixture of secretory protein and polysaccharide, infers intestinal anchorage ability to the bacteria; therefore, by altering biofilm production in the presence of chitosan, surface encapsulation was measured following the method described earlier with certain modifications (*25*). For doing that, 200 μl of MRS broth

containing freshly prepared culture (OD 0.6) of *L. reuteri* was seeded to each well of 96-well plates along with medium blank. Then, different concentrations of chitosan (0.00, 0.02, 0.04, 0.05, 0.06, and 0.08 mg/ml) were added to each well and incubated statically for 24 and 48 hours at 37°C, pH 6.5. The supernatants were discarded without disrupting the biofilm, followed by the addition of 10 μl of 0.5% crystal violet (w/v) solution to each well and incubation for 10 min at room temperature. Following incubation, excess crystal violet solution was removed by washing with distilled water (twice). After that, 200 μl of 100% ethanol was added to each well, and OD was taken at 570 nm and plotted as percentage of biofilm production per unit weight of bacteria and against concentrations of chitosan (*25*, *26*). To avoid any disruption of the biofilm production, the samples were handled delicately.

The production ability of biofilm by BB in SGF and SIF

Fresh *L. reuteri* culture was taken, and BBs were synthesized using the earlier protocol. BBs (1×10^6) were then seeded in 96-well plates in the presence of 300 μl of 1× MRS medium at SGF (pH 2.0) or SIF (pH 6.4 and 7.4) in the presence or absence of pepsin and pancreatin for SGF and SIF, respectively. After that, the plates were incubated for 24, 48, and 72 hours at 37°C in static conditions. After incubation, plates were processed as before and calculation was done using OD at 570 as percentage of biofilm production per unit weight of BBs (*26*).

Stability and structural integrity of BB in SGF and SIF

To determine the structural stability of the mesoporous nanoparticles on the bacterial surface, FUBBs were incubated for 72 hours at 37°C with constant stirring at 60 rpm in SGF (pH 2.0) and SIF (pH 6.4 and pH 7.4) in the presence of pepsin (SGF) or pancreatin (SIF). Sampling was done at different time points (0-, 12-, 24-, 48-, and 72-hour intervals) and was monitored under FE-SEM following the same protocol as before.

Animal experiment

An in-bred strain of Swiss albino mice, *Mus musculus*, weighing 30 ± 5 g at the initiation of the experiment, was reared and maintained in the animal house of the Chittaranjan National Cancer Institute (CNCI), Kolkata. The animal house was kept clean, hygienic, and disinfected as per the regulations of the Animal Ethics Committee, Government of India. The animals were maintained at an ambient temperature of 24 ± 1°C in 12-hour light and 12-hour dark cycles. Mice were allowed standardized pelleted food and pure and healthy drinking water ad libitum. The institutional animal ethical committee has approved the protocol (no. IAEC-1774/BB-6/2020/6).

Adsorption on BBs on the GI tract of mouse ex vivo

Three healthy adult male Swiss albino mice were euthanized, and the small stomach and intestinal regions were collected. After that, the collected intestinal regions were washed thoroughly with sterile PBS to clean any fecal residuals, cut into small pieces (approximately 5 mm by 5 mm), and incubated in 5% povidone-iodine solution for 15 min for disinfection. The tissue was then thoroughly washed with sterile PBS and floated on Dulbecco's modified Eagle's medium (pH 7.4) with 10% serum in a 96-well plate. 25 μl of each of the following samples—(1×10^7 cells/ml) *L. reuteri*, BBs, and Rd (0.1 mg in 100 mg of BB concentration)-loaded BBs—were placed on intestinal tissue in a 96-well plate. After 30 min of incubation, tissue samples were washed thoroughly with sterile PBS 10 times before processing for confocal and FE-SEM analysis. Fluorescence analysis was done in 96-well fluorescence plates, one section in each good format, and data were collected after excitation at 485 nm. For FE-SEM, after incubation and thorough washing, tissue section was fixed using 4% glutaraldehyde solution for 2 hours at 4°C. Then, dehydration of tissues was done using an ethanol gradient (50, 70, 75, 90, 95, and 100%) treatment, 20 min each. After gold coating, the samples were processed for FE-SEM, as mentioned above.

Liquid chromatography–electrospray ionization–mass spectrometry analysis for detecting 5-FU $[M\text{-}H]^+$ abundance from peak intensity

Sample preparation

The sample was prepared using the protocol described previously, where 100 μl of the murine plasma sample was mixed with 10 μl of glacial acetic acid and 1 ml of ethyl acetate (*18*). The resulting mixture was vortexed for 10 min and then centrifuged for 5 min at 13,000*g* at room temperature. The supernatant was transferred to 1.5-ml Eppendorf tubes and evaporated to dryness using a SpeedVac vacuum concentrator (Thermo Fisher Scientific). The dried residues were reconstituted in 100 μl of acetonitrile/water/formic acid (97:3:0.1, v/v/v), vortexed for 10 s, and transferred to autosampler vials. Vials were then placed into the autosampler (kept at 4°C), and 10 μl from each vial was injected. The samples were prepared in independent replicates.

Chromatography and mass spectrometry

The liquid chromatography (LC) system (Xevo G2-XS QToF, Waters, Milford, MA, USA) consisted of an autosampler with a binary pump, a C18 BEH column 1.7 μm, 1 mm by 100 mm dimension, and an isocratic flow of isoamyl alcohol. Mobile phase solvent A consisted of 0.1% (v/v) formic acid in water, and mobile phase solvent B consisted of 0.1% (v/v) formic acid in acetonitrile. The initial mobile phase composition was 95% solvent A and 5% solvent B pumped at a flow rate of 40 μl/min for 7 min. From 7 to 8 min, solvent A was decreased from 95 to 65%, and solvent B was increased from 5 to 30%, with the same flow rate. From 8 to 10 min, solvent A was decreased to 15%, and solvent B was kept at 85%. The overall run time was 10 min, with a flow rate of 40 μl/min. Mass spectrometric (MS) detection was carried out using a Waters Xevo G2-XS QToF mass spectrometer connected to the ACQUITY UPLC H-Class System (Waters, Milford, MA, USA) via ZSpray dual orthogonal spray source. Electrospray ionization (ESI) was operated in positive-ion, MS-MS (MS^E) mode. The mass spectrometer settings were kept as follows: capillary voltage, 3 kV; cone voltage, 30 V; source temperature, 100°C; and desolvation temperature, 250°C. The cone and desolvation gas flows were kept at 50 and 300 liters/hour, respectively. The ramp collision voltage was 18 to 40 V. The instrument was calibrated with sodium formate to achieve mass accuracies of <0.5 mDa. Internal calibration was performed with reference (lock mass), where leucine enkephalin was used. Its mass of 556.2771 was calibrated within 10-ppm (parts per million) error to ensure mass accuracies and reproducibility of the optimized MS conditions. The LC system and mass spectrometer were controlled by Waters MassLynx software (version 4.0), and the 5-FU $[M\text{-}H^+]$ peak intensity at 131 (molecular weight of $[M\text{-}H^+]$) was collected using the same software. The relative abundance of 5-FU $[M\text{-}H^+]$ was plotted as means ± SE at different time points concerning the untreated murine plasma, which served as a control.

qPCR analysis

Oral gavaging of vancomycin + neomycin + ampicillin + metronidazole + gentamicin at 200 μl of 1.0 g/liter each for 3 days was applied to deplete intestinal microbiota. One group of animals received BB by oral gavaging. Another group remains untreated. After 8 hours, intestinal tissue samples from both groups of animals were collected and homogenized for qPCR analysis. gDNA was extracted from the homogenized murine intestine samples (control with antibiotic treated and antibiotic + BB treated) using the Takara NucleoSpin Tissue Kit, following the manufacturer's protocol. The concentration of the extracted gDNA was measured using a NanoDrop spectrophotometer. To check the presence of BB attached to the intestine wall, *L. reuteri*–specific gene primers were designed using PREMIER Biosoft software and tested for efficacy by performing normal PCR analysis. To determine the relative abundance of *L. reuteri*, qPCR was performed. qPCR analysis was carried out with Takara TB Green Premix Ex Taq II (Tli RNaseH Plus) using the CFx96 Touch Real-Time PCR machine (Bio-Rad). The following program was performed: 3 min at 98°C, 40 cycles of 10 s at 95°C, and 15 s at 50°C. The CFX Maestro software automatically determined the Cq (quantification cycle) values after 40 cycles, followed by melt curve analysis. The Cq values obtained for *L. reuteri*–specific genes were normalized against the abundance of the 16*S* rDNA gene, which remains conserved for different lactobacillus species present in the murine intestine. The relative abundance of *L. reuteri* in the intestine was calculated using the Livak $2^{-\Delta\Delta CT}$ method, using 16*S* rDNA as the reference gene. For each gene, the analysis was carried out for at least three replicates.

Primers used for qPCR analysis are as follows: *L. reuteri* specific, 5′-TGATGATGAAGTGCGGC-3′ (forward) and 5′-CGTCATTAAACAAGCTGAGAAT-3′ (reverse); *Lactobacillus* 16*S* rDNA, 5′-CGCCTGGGGAGTACGA-3′ (forward) and 5′-CTGGTAAGGTTCTTCGC-3′ (reverse).

Mouse model of tumor and treatments

S180 cells were injected into the peritoneal cavity of the mice and proliferated to produce ascites. The cell colonies were maintained by weekly transplantation of the tumor cells from the ascitic fluid into the peritoneal cavity of another mouse. S180 cells were isolated from the ascitic fluid and suspended in PBS. A total of 36 Swiss albino mice at the age of 5 to 6 weeks were injected with 5×10^6 cells (in 100 μl of PBS) into the right leg flank. After 10 days, when the palpable tumor was observed, all mice were divided into six groups (six mice in each group) as follows: (i) vehicle control (saline-treated), (ii) EBB, (iii) FU-25, (iv) FUBB-25, (v) FU-50, and (vi) FUBB-50. The solution was centrifuged in two separate vials at 1000 rpm for 2 to 3 min, and the supernatant was discarded. FUBB-25 and FUBB-50 solutions were prepared by resuspending 5-FU with the pellet to get the effective concentration of 25 mg/kg BW and 50 mg/kg BW, respectively, at the time of oral gavaging. For survival analysis, another 36 Swiss albino mice (6 mice in each group) were injected with 5×10^6 cells (in 100 μl of PBS) into the peritoneal cavity for ascites tumor. All groups of animals (both solid and ascites tumors) were orally administrated with drugs and on days 1, 4, 7, and 10 and observed for 30 days.

In vivo tumor regression and survivability study

Tumor volumes were measured for 29 days from the day of initiation of treatment. The tumors were measured with a Vernier caliper in 3 days to determine the shortest diameter (A) and the longest diameter (B). The volume was then calculated by using the formula $V = (A^2B)/2$. Data were analyzed for statistical significance using Student's *t* test. A value of $P \leq 0.05$ was considered statistically significant. Mice were euthanized after 29 days of tumor transplant, and tumors and organs were collected for histopathological analysis. The relative tumor volume (RTV) on day *n* was calculated using $RTV = TV_n/TV_0$, where TV_n is the tumor volume on day *n* and TV_0 is the tumor volume on day 0. The following formula calculated tumor growth inhibition rate (TIR): TIR = {(1 − (mean volume of treated tumors)/mean volume of control tumors)} × 100% (*27*). Kaplan-Meier survival analysis was used to calculate the statistical differences in survival between different groups of tumor-bearing mice.

Histopathological analysis

All the specimens (tumor, liver, and kidney tissues) were washed carefully in PBS and fixed in 10% neutral buffered formalin within 30 min after resection. After 24 hours, tissues were immersed into increasing alcohol concentration, i.e., alcohol gradation as 50, 70, 90, and 100% ethanol for 30 min each. Then, the specimens are placed into xylene for 15 to 20 min to displace the alcohol from the tissue. Tissues were placed into liquid wax (65°C) for 4 hours in the oven to maintain a constant temperature. Tissue blocks were prepared, and 5-μm sections were cut and placed onto poly-L-lysine–coated slides. For staining, slides containing sections were placed in xylene to remove wax. Slides were then placed into decreasing alcohol concentration (100, 90, 70, and 50% ethanol) for 10 min each. Then hematoxylin stain was applied for 3 min. Slides were then placed in 70 and 90% ethanol for 5 min each. After that, the eosin stain was applied for 1 min. Slides were then passed through increasing alcohol concentration (90 and 100% ethanol). Slides were then kept into xylene for 10 min, mounted with DPX mountant (a mixture of distyrene, a plasticizer, and xylene), and observed in different magnifications under a bright-field microscope.

Evaluation of hepatic and renal biochemical parameters

To understand the effect on hepatic and renal biochemical parameters, if any, by BB alone or combined with different 5-FU doses, blood from all groups of animals was collected on the 29th day. Blood was placed in a centrifuge tube for 30 min and then centrifuged at 3000 rpm for 10 min, and serum was collected. Then, cholesterol, triglycerides, SGOT, and SGPT were estimated from the serum sample using the fully automatic analyzer (Cobas Integra 400, Roche) method. For estimation of total cholesterol, the analyzer measured the formation of red quinone imine dye at 540/600 nm. A decrease in absorbance in 340 nm was measured for SGOT and SGPT levels in the blood (*28*). For serum albumin analysis, the bromocresol green method was adopted. The automatic analyzer also measured serum bilirubin, globulin, creatinine, and alkaline phosphatase.

Measurement of host immune response against BB-mediated drug delivery

To understand the immune response of the BB-mediated drug delivery, the total count of blood cells and cytokine IL-6 and IL-10 expression have been studied in the mice after 2 weeks of treatment. Two treatment groups, i.e., FU-50 and FUBB-50 and control consisting of six Swiss albino mice in each (without tumor), were taken for this study. The animals were orally administered with 5-FU (50 mg/kg BW, FU-50) alone or through BB as a drug carrier. The

drug dose was given on the 1st, 4th, 7th, and 10th days of treatment, and blood samples were analyzed on the 15th day of treatment. First, blood samples were collected in EDTA-coated vials. The number of red blood cells, leukocytes, and platelets in the blood of mice was measured with an autoanalyzer. Further, to determine the serum cytokine (IL-6 and IL-10) levels, mouse-specific ELISA kits (Invitrogen, KMC0061, and R&D Systems, M1000B) were used.

Statistical analysis

All data were analyzed using Student's *t* test and one-way and two-way analysis of variance (ANOVA) followed by Tukey's multiple comparison test. The Kaplan-Meier survival analysis and the log-rank test were conducted for survival analysis.

SUPPLEMENTARY MATERIALS

Supplementary material for this article is available at https://science.org/doi/10.1126/sciadv.abh1419

REFERENCES AND NOTES

1. S. A. Agnihotri, N. N. Mallikarjuna, T. M. Aminabhavi, Recent advances on chitosan-based micro- and nanoparticles in drug delivery. *J. Control. Release* **100**, 5–28 (2004).
2. R. N. Gursoy, S. Benita, Self-emulsifying drug delivery systems (SEDDS) for improved oral delivery of lipophilic drugs. *Biomed. Pharmacother.* **58**, 173–182 (2004).
3. P. K. Kondamudi, R. Malayandi, C. Eaga, D. Aggarwal, Drugs as causative agents and therapeutic agents in inflammatory bowel disease. *Acta Pharm. Sin. B* **3**, 289–296 (2013).
4. M. Shale, G. G. Kaplan, R. Panaccione, S. Ghosh, Isotretinoin and intestinal inflammation: What gastroenterologists need to know. *Gut* **58**, 737–741 (2009).
5. S. Y. Shaw, J. F. Blanchard, C. N. Bernstein, Association between the use of antibiotics and new diagnoses of Crohn's disease and ulcerative colitis. *Am. J. Gastroenterol.* **106**, 2133–2142 (2011).
6. É. Toussirot, É. Houvenagel, V. Goëb, D. Fouache, A. Martin, P. Le Dantec, E. Dernis, D. Wendling, T. Ansemant, J. M. Berthelot, B. Bader-Meunier, B. Kantelip, Development of inflammatory bowel disease during anti-TNF-α therapy for inflammatory rheumatic disease: A nationwide series. *Joint Bone Spine* **79**, 457–463 (2012).
7. J. Davies, Origins and evolution of antibiotic resistance. *Microbiologia* **12**, 9–16 (1996).
8. M. Qiao, G. G. Ying, A. C. Singer, Y. G. Zhu, Review of antibiotic resistance in China and its environment. *Environ. Int.* **110**, 160–172 (2018).
9. H. Hillaireau, P. Couvreur, Nanocarriers' entry into the cell: Relevance to drug delivery. *Cell. Mol. Life Sci.* **66**, 2873–2896 (2009).
10. Y. Zhang, H. F. Chan, K. W. Leong, Advanced materials and processing for drug delivery: The past and the future. *Adv. Drug Deliv. Rev.* **65**, 104–120 (2013).
11. A. C. Krauss, X. Gao, L. Li, M. L. Manning, P. Patel, W. Fu, K. G. Janoria, G. Gieser, D. A. Bateman, D. Przepiorka, Y. L. Shen, S. S. Shord, C. M. Sheth, A. Banerjee, J. Liu, K. B. Goldberg, A. T. Farrell, G. M. Blumenthal, R. Pazdur, FDA approval summary: (Daunorubicin and cytarabine) liposome for injection for the treatment of adults with high-risk acute myeloid leukemia. *Clin. Cancer Res.* **25**, 2685–2690 (2019).
12. D. Akin, J. Sturgis, K. Ragheb, D. Sherman, K. Burkholder, J. P. Robinson, A. K. Bhunia, S. Mohammed, R. Bashir, Bacteria-mediated delivery of nanoparticles and cargo into cells. *Nat. Nanotechnol.* **2**, 441–449 (2007).
13. M. L. Hans, A. M. Lowman, A dual-responsive mesoporous silica nanoparticle for tumor-triggered targeting drug d for drug delivery and targeting. *Curr. Opin. Solid State Mater. Sci.* **6**, 319–327 (2002).
14. D. A. MacKenzie, F. Jeffers, M. L. Parker, A. Vibert-Vallet, R. J. Bongaerts, S. Roos, J. Walter, N. Juge, Strain-specific diversity of mucus-binding proteins in the adhesion and aggregation properties of *Lactobacillus reuteri*. *Microbiology* **156**, 3368–3378 (2010).
15. J. F. Sicard, G. Le Bihan, P. Vogeleer, M. Jacques, J. Harel, Interactions of intestinal bacteria with components of the intestinal mucus. *Front. Cell. Infect. Microbiol.* **7**, 1–2 (2017).
16. F. Imperi, E. V. Fiscarelli, D. Visaggio, L. Leoni, P. Visca, C. Juan, Activity and impact on resistance development of two antivirulence fluoropyrimidine drugs in *Pseudomonas aeruginosa*. *Front. Cell. Infect. Microbiol.* **9**, 1–11 (2019).
17. J. B. Navarro, L. Mashburn-Warren, L. O. Bakaletz, M. T. Bailey, S. D. Goodman, Enhanced probiotic potential of *Lactobacillus reuteri* when delivered as a biofilm on dextranomer microspheres that contain beneficial cargo. *Front. Microbiol.* **8**, 489 (2017).
18. J. E. Kosovec, M. J. Egorin, S. Gjurich, J. H. Beumer, Quantitation of 5-fluorouracil (5-FU) in human plasma by liquid chromatography/electrospray ionization tandem mass spectrometry. *Rapid Commun. Mass Spectrom.* **22**, 224–230 (2008).
19. P. Kaur, D. Choudhury, Universal delivery system for drugs/molecules of choice using live microbes and method thereof, Indian Patent No. 201911027084 (2019).
20. M. Motiei, S. Kashanian, Novel amphiphilic chitosan nano-carriers for sustained oral delivery of hydrophobic drugs. *Eur. J. Pharm. Sci.* **99**, 285–291 (2017).
21. V. Zamora-Mora, M. Fernández-Gutiérrez, Á. González-Gómez, B. Sanz, J. S. Román, G. F. Goya, R. Hernández, C. Mijangos, Chitosan nanoparticles for combined drug delivery and magnetic hyperthermia: From preparation to in vitro studies. *Carbohydr. Polym.* **157**, 361–370 (2017).
22. M. Marques, Dissolution media simulating fasted and fed states. *Dissolution Technol.* **11**, 16 (2004).
23. E. Piórkowska, M. Kaza, J. Fitatiuk, I. Szlaska, T. Pawiński, P. J. Rudzki, Rapid and simplified HPLC-UV method with on-line wavelengths switching for determination of capecitabine in human plasma. *Pharmazie* **69**, 500–505 (2014).
24. V. Helen Shiphrah, S. Sahu, A. Ranjan Thakur, S. Ray Chaudhuri, Screening of bacteria for lactic acid production from whey water. *Am. J. Biochem. Biotechnol.* **9**, 118–123 (2013).
25. C. Bhattacharyya, U. Bakshi, I. Mallick, S. Mukherji, B. Bera, A. Ghosh, Genome-guided insights into the plant growth promotion capabilities of the physiologically versatile *Bacillus aryabhattai* strain AB211. *Front. Microbiol.* **8**, 1–16 (2017).
26. M. C. Leccese Terraf, M. S. Juárez Tomás, L. Rault, Y. Le Loir, S. Even, M. E. F. Nader-Macías, Biofilms of vaginal *Lactobacillus reuteri* CRL 1324 and *Lactobacillus rhamnosus* CRL 1332: Kinetics of formation and matrix characterization. *Arch. Microbiol.* **198**, 689–700 (2016).
27. M. Nukatsuka, F. Nakagawa, T. Takechi, Efficacy of combination chemotherapy using a novel oral chemotherapeutic agent, TAS-102, with oxaliplatin on human colorectal and gastric cancer xenografts. *Anticancer Res.* **35**, 4605–4615 (2015).
28. S. Chowdhury, P. P. Chakraborty, Universal health coverage—There is more to it than meets the eye. *J. Fam. Med. Prim. Care.* **6**, 169–170 (2017).

Acknowledgments: We thank S. Roy (Bose Institute, Kolkata) for assistance in acquiring the MS data. B.B. wants to thank the director of CNCI for institutional funding and infrastructural support. **Funding:** D.C. is thankful to the DST/SERB project (ECR/2016/000486) for funding. P.K. is grateful to DST, Government of India, for a fellowship under ECR/2016/000486 (project). A.G. acknowledges the SERB, Government of India (CRG/2018/001732), for extramural funding and Bose Institute, Kolkata, for infrastructural support. S.D. is thankful to the CSIR, Government of India, for fellowship [09(0667/11122)/2021-EMR-I]. N.G. would like to acknowledge Science and Engineering Research Board Grant, India, for grant ECR/2017/00092. N.G. would like to acknowledge BHU for seed grant. **Author contributions:** Conceptualization: D.C. Methodology development: P.K. Data collection: P.K., S.G., A.B., and K.G. Data analysis: P.K., S.G., A.B., D.C., and B.B. Supervision: D.C., B.B., A.G., and N.G. Visualization: P.K., S.G., and A.B. Writing original draft: P.K. Revision works: P.K., S.G., A.B., and S.D. Review and editing: P.K., S.G., A.B., S.D., A.G., R.L.M., B.B., and D.C. Manuscript validation: P.K., S.G., A.B., K.G., S.D., A.G., N.G., R.L.M., B.B., and D.C. Funding acquisition: D.C., A.G., S.D., and N.G. **Competing interests:** P.K. and D.C. are inventors on a patent related to this work filed by Thapar Institute of Engineering and Technology (no. 201911027084, filed on 7 May 2019, published on 1 August 2021). The authors declare no other competing interests. **Data and materials availability:** All data needed to evaluate the conclusions in the paper are present in the paper and/or the Supplementary Materials.

Submitted 18 February 2021
Accepted 22 January 2022
Published 11 March 2022
10.1126/sciadv.abh1419